Estimating lighting device inventories with the LANcube v2 multiangular radiometer

Martin Aubé[1,2,3], Julien-Pierre Houle[2]

[1] Département de physique, Cégep de Sherbrooke

[2] Département de géomatique appliquée, Université de Sherbrooke

[3] Physics Department, Bishop's University

Correspondence: martin.aube@cegepsherbrooke.qc.ca; Tel.: 1-819-564-6350 #4146

Current address: 475 rue du Cégep, Sherbrooke, Québec, Canada J1E 4K1

Abstract:
This paper is a technical report describing the use of an open-source instrument called LANcube v2 to estimate a lighting devices inventory. The instrument has 5 color sensitive sensors, each on a face of a cube. The instrument can be mounted on a car roof to create a map of the artificial light at night while roaming the streets and roads. Based on the temporal variations of the detected signal on various cube's faces, we developed a method of finding the approximate position in 3D of each source. The lamp spectral types can be determined relatively well thanks to the color balance of the raw Red (R), Green (G), Blue (B), and Clear (C) color bands. If one assumes a typical angular photometry of a source with respect to its location, it is possible to estimate roughly its current luminous flux. Such information allows us to build a lighting devices inventory of a territory. One advantage of that new method is that it can provide information about the private sources that are always excluded from public lighting inventories. We compared the inventory extracted with that new methodology with an in-situ lamp inventory made for two villages in Canada. This comparison allows us to emphasize the strengths and limitations of the method by comparing to the ground truth. We found that we were able to detect 99% of the sources with flux higher than 1000 lumen and located within 15 meters from the road. We also found that we generally overestimate the height of the devices by 21 to 51% depending on the lamp photometry. This overestimate surely reflects in an overestimate of the fluxes. Finally, we found that the proposed method is very efficient to recognize the spectral type of the devices with 99% of success.

Keywords: Remote sensing; Night; Light pollution; streetlight; radiometer; Lighting devices inventory

---

1 Introduction

In the recent years, obtrusive light has been found to affect the entire environmental equilibrium. The Artificial Light at Night (ALAN) can perturb health of many species (animals, insects, and plants) including humans [1-7]. ALAN can be divided into two main components the direct and indirect ALAN. Indirect ALAN is the component reaching the environment after scattering in the atmosphere. This component is often referred as artificial sky brightness. Many instruments and methods have been used to monitor the artificial sky brightness [8]. On the other hand, direct ALAN does not interact significantly with the atmosphere and therefore reach almost directly the environment. This component is often referred as obtrusive light. The latter component is many orders of magnitude higher than the indirect component for urban environments or for sites located within a few tens of meters to a source. To better model and monitor the direct component of ALAN in real environments, there is a need to develop methods for estimating lighting inventories using non imaging devices.

In order to study the biological effects of ALAN, it is required to monitor it through color sensitive measuring devices. The spectral content or color of the ALAN is important because that many biological processes involved in the ALAN induced perturbations are wavelength dependent [9, 10, 11]. But not only the spectrum matters, the orientation of the light propagation too. Ideally, the measuring devices must be multispectral and multiangular. In

the present work, we describe the use of such a sensor called LANcube [12, 13] to characterize the properties of lighting devices located within 15 meters of a road or street.

To get even more detailed information on the effect of the ALAN, one promising approach if to use radiative transfer models [14]. But modeling of the obtrusive light during the night requires the knowledge of many environmental parameters. Among the most important to know are the source positions, spectral types, luminous fluxes, and angular emission functions. In this paper, we show how the analysis of the data recorded by the LANcube v2 may deliver at least an estimation of most of these variables. To achieve that, the LANcube v2 needs to be installed on top of a vehicle roaming streets and roads. In our methodology, we assume that the angular emission function of the source is isotropic. That is of course a major weakness of the method which in general implies an overestimation of the lamp height and of the distance to the source. The examination of many streetlight photometric Illuminating Engineering Society (IES) files showed us that the approximation is better for old High Intensity Discharge (HID) technology than for the LED technology. The typical span of increase of the emission functions toward larger nadir angles for LED streetlights, result in larger overestimates of the height and lateral distance. In the future, we plan to replace the isotropic model by an average of emission functions of typical lighting devices expected to be found in the studied area. Such an improvement may reduce the overestimates.

2 The LANcube v2 device

The LANcube is a device designed to sample the multispectral and multiangular properties of the direct ALAN. The LANcube is a cube-shaped system having a 4-color band sensor on five of its faces. The sensors are TCS34725 Color Light-to-Digital Converter. The latest version (v2) of the LANcube v2 has shorter acquisition time than the original version. In the darkest conditions, it can read the 5 sensors every 0.6 seconds. This acquisition rate allows to monitor the temporal change in illuminance reaching the sensor while in movement. Given that the LANcube v2 also comprise a Global Positioning System (GPS), its position can be recorded at each sensor reading. The temporal and positional information can be combined to infer the properties of the sources encountered along the path.

The LANcube v2 is equipped with a WIFI interface which allows an access to the data from a mobile device. The LANcube v2 is developed in an open science approach so that the recipe to build the LANcube v2 along with its software is released under open licenses [13]. For a better power stability, the LANcube v2 has an integrated Uninterruptible Power Supply (UPS). The picture of LANcube v2 is shown in Figure 1. In addition to position and time information, the LANcube v2 provides many parameters in real time:

- the uncalibrated R, G, B, and C color irradiances
- the Correlated Color Temperature (CCT)
- the Melatonin Suppression Index (MSI)
- the illuminance in lux

Figure 1. The LANcube v2 radiometer. On the bottom of the left face, are the USB and ethernet ports and on the right face one can see the operating switch and status RGB LED. At the center of each face lies a light color sensor (TCS 34725) that can measure both irradiances and illuminance. The size of the LANcube v2 is 9x9x9 cm.

3 Analysing the signal recorded by the LANcube v2

Thanks to its high sampling frequency, it is now possible to extract spatial information about the sources out of the temporal variations of the LANcube v2 sensor's signals. To do so, the LANcube v2 needs to be moved. This is usually done while the LANcube v2 is installed on top of a vehicle roaming along the roads and streets. In this section we will derive the equations allowing to determine approximately the position, height, spectral type and luminous flux of the sources located along or nearby a street or a road.

In this method, we exploit the two lateral sensors along with the top sensor. As for the LANcube v2 sensor numbering, the sensor on the side that is on the right when one is looking forward is sensor #3, the opposite face holds sensor #5 while the top face holds sensor #1.

The idea behind the detection of the lighting devices relies on the temporal analysis of sensors illuminance along the LANcube v2 trajectory. The problem splits into five cases because that the source may be directly above, completely on the right-handed or left-handed side or above in an oblique direction on each side.

3.1 Lighting devices spectral type recognition

To determine the spectral type, we make use of the color ratios relatives to the green channel in order to determine the coordinate of the source in a ad hoc 3D color space defined by the red/green, blue/green and infrared/green color ratios (r/g,b/g andi/g). r, g, b and i are derived from the raw red, green, blue and clear channels (R, G, B, C) as explained in [12]. Basically, we first use the sum of the 3 colors and the clear channel to get an estimate of the near infrared$i$. Then we correct the raw colors (R, G, B) channels by subtracting the infrared estimate to get the infrared-free colors (r, g, b).

We recorded the light with the LANcube v2 for many reference lamps of different typical lamp spectral types. We actually sampled High Pressure Sodium (HPS), Metal Halides (MH), Mercury Vapor (MV), Light-Emitting Diodes (LED) at different Correlated Color Temperature (CCT), and Incandescent (INC). This allows to map in the 3D color space different positions for a variety of the targeted technologies (or spectral types). That database is given in Table 1. The content of the table will evolve in the future as long as new lamps will be identified and sampled. This is important because lamps of the same spectral type can have various spectral power distribution and therefore different positions in the color space.

The spectral type of a given source detected by the LANcube v2, is identified by finding the smallest distance ($\delta_{min}(s)$) out of the distances relative to each lamp ($\delta(s)$, see equation 1) type of Table 1 in the ad hoc 3D color space defined by the color ratios r/g , b/g , and i/g. Note that the r/g ratios are multiplied by a factor of 0.14 which showed experimentally to better discriminate the different technologies because that the span of values observed for that ratio is larger than the two others (without considering the incandescent that has a very high i/g ratio). We actually used this *ad hoc* color space instead of well-known models like CIE1931 XYZ model because that in our case the addition of the near infrared signal help discriminates technologies having similar visible colors. For some LED spectra, the i/g ratio can be negative. It simply reflects the complex combination of the spectra and the bands spectral sensitivities. In other words, i is not really a pure infrared signal but is still useful to better discriminate spectral types.

$$\delta(s)^2 = 0.14^2([r/g] - [r/g]_s)^2 + ([b/g] - [b/g]_s)^2 + ([i/g] - [i/g]_s)^2 \quad (1)$$

In equation 1, s stands for the elements of the database of Table 1.

Table 1. Coordinates of the various typical lamp spectrum in the ad hoc 3D color space. *u* stands for Upward Light Output Ratio (ULOR)

$[r/g]_s$	$[b/g]_s$	$[i/g]_s$	u	Spectral type
2.64	0.60	0.07	0.03	HPS
2.50	0.65	0.07	0.03	HPS
2.79	0.59	0.16	0.03	HPS
3.47	0.74	0.25	0.03	HPS
2.50	0.77	0.11	0.03	HPS
2.27	0.84	0.50	0.03	HPS
2.21	0.67	0.07	0.03	HPS
2.84	0.71	0.16	0.03	HPS
0.87	0.98	0.22	0.05	MH4000
0.80	0.54	0.15	0.10	MV
1.01	0.57	0.36	0.10	MV
5.43	0.64	0.17	0.00	LED1500
1.94	0.42	-0.11	0.00	LED1650
1.64	0.38	-0.08	0.00	LED1650
3.87	0.47	0.13	0.00	LED1800
2.65	0.43	-0.10	0.00	LED1800
2.37	0.44	-0.15	0.00	LED1800
3.42	0.51	0.03	0.00	LED1800
2.91	0.49	0.01	0.00	LED1800
1.85	0.56	0.03	0.00	LED2200
1.99	0.75	0.04	0.00	LED3000
1.87	0.69	0.02	0.00	LED3000
0.81	0.51	-0.11	0.00	LED3500
1.04	0.77	-0.03	0.00	LED4000
1.00	0.67	-0.06	0.00	LED4000
0.95	0.58	-0.09	0.00	LED4000
1.21	0.89	0.02	0.00	LED5000
0.99	0.84	0.02	0.00	LED5500
0.60	0.81	-0.09	0.00	LED5500
3.38	0.83	3.65	0.30	INC2550
2.79	0.82	2.37	1.30	INC2550

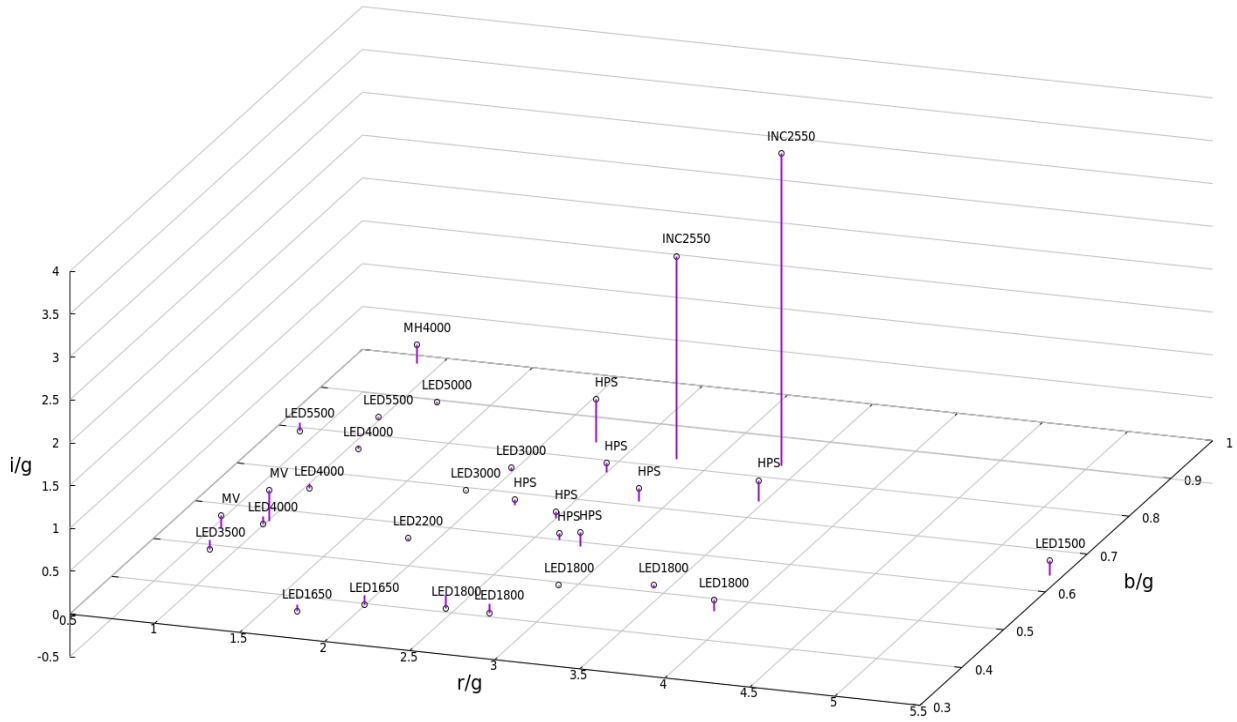

Figure 2. Lamp spectra in the *ad hoc* color space. The purple lines, showing the *i/g* component, clearly indicate how this axis helps to discriminate incandescent lamps (INC2550) from other spectral types.

3.2 Lighting devices position

One of the first treatment applied to the temporal signals of the sensors is a gaussian filter in order to reduce noise and cosmic rays peaks. That filtering step also smooth the signals so that peaks in the signals may happen between two measured points. When looking at the temporal signal of sensors #1, #3 and #5, one should note that at some moments the signals reach a local maximum and then decline until another maximum is observed. The maximum signal indicates that the LANcube v2 is located almost aside and or below a source. If we detect only a maximum on sensor #1 that means that the source is located directly above the LANcube v2. On the other hand, if the maximum is only on the #3 or #5, the source is located on the side at about the same height or below the LANcube v2 height. A peak on sensor #3 means a source on the right side of the car while on sensor #5 it is located on the left side. If the maximum on sensor #1 coincide with a maximum on sensors #3 or #5, the lamp is higher to the LANcube v2 on the side.

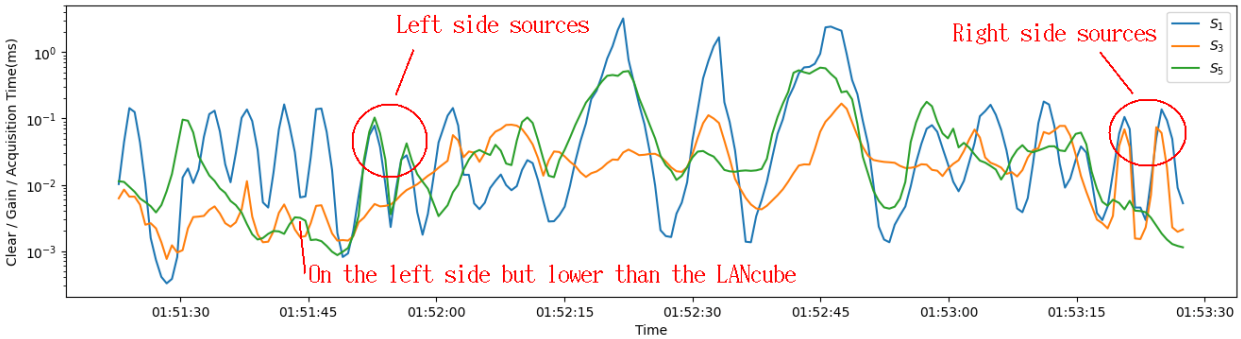

Figure 3: Typical signal recorded by the LANcube v2 as a function of time on sensors 1, 3, and 5 in a part of Saint-Camille, Canada. We used a vertical log scale to show both the dim and luminous sources. We highlighted two sets of coincident peaks with red circles. The first one detetected on the right side and the second one, on the left side of the car. For these two cases, the fixtures were higher than the LANcube and this is why we detected the peaks on a side sensor and on the top simultaneously. We also show an example of a fixture lower than the LANcube located on the left side of the car.

3.3 Removing the background light

Given that we are only interested in the detection of the direct light coming from a nearby source, we need to remove the light reaching a sensor after a reflection on surfaces (facades or ground). This is done independently for each sensor. To do so we are using a 7 data sliding window, keeping the minimum value. The minimum value is simply removed from the original signal. We therefore obtain the cleaned illuminance for sensors #1, #3 and #5, respectively denoted $E_{v1}(t)$, $E_{v3}(t)$ and $E_{v5}(t)$. In the method described in this paper we assume that the light reaching a sensor is dominated by the nearby source and therefore the farther sources have negligible effect on the signal. For typical streetlight in Canada, this is correct since when then sensor is in front of a source its distance is about 7 meters while the next one is generally 30 to 60 meters away. That means that the next source has an approximate maximum relative effect of $(7/30)^2$, i.e., about 5% of the signal detected and this is maximum value because we do not account for the angular projection which reduce significantly the signal coming for the remote source.

3.4 Case 1: lighting device higher than the LANcube v2 on the side

To simplify the discussion, we will focus on sensors #1, #3 which are related to a detection above or on the right side. But the same analysis may be done with the left side simply by replacing sensor #3 by sensor #5.

When maximums on E_{v1} and E_{v3} coincide in time, it means that we are aside a source higher than the LANcube v2. In that case, we have enough data to determine the source position relative to the LANcube v2 position.

Figure 4 illustrates the geometry of a typical street with a source higher than the LANcube v2 and on the side. In that figure, h is the height of the LANcube v2 relative to the street, H the height of the source, d is the horizontal distance between the source and the LANcube v2, and θ is the nadir angle of the line from the source to the LANcube v2.

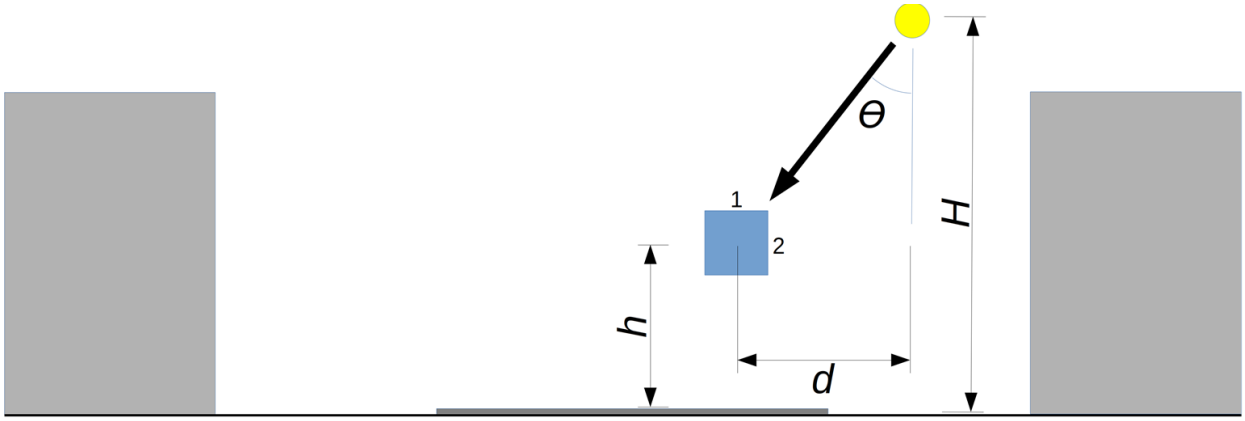

Figure 4: Geometry of a street. The gray rectangles represent buildings, while the blue square is the LANcube v2 and the yellow circle is a source.

Since the sensor angular sensitivities are very close to a cosine function, we can express the local maximum signals as a function of the illuminance normal to the direction of the source $E_{v\perp}$. This gives Equation 2 for the upper sensor illuminance E_{v1}, and 3 for the side sensors illuminance E_{v3}.

$$E_{v1} = E_{v\perp}\cos(\theta) \quad (2)$$

$$E_{v3} = E_{v\perp}\cos(\pi - \theta) = E_{v\perp}\sin(\theta) \quad (3)$$

Simple geometry allows to formulate the following relationship linking the nadir angle from the source to the sensor θ as a function of the horizontal distance between the source to the sensor d, the height of the source H and the height of the sensor h.

$$\tan(\theta) = \frac{d}{H-h} \quad (4)$$

With the definition of a tangent along with Equations 2 and 3 we can write:

$$\tan(\theta) \equiv \frac{\sin(\theta)}{\cos(\theta)} = \frac{E_{v3}}{E_{v1}} \quad (5)$$

We assume that h is known. After combining Equations 4 and 5, we obtain:

$$H - h = d\frac{E_{v1}}{E_{v3}} \quad (6)$$

From figure 4, we can write the following expression if the LANcube v2 moved of a distance D along the street. If we also assume that between the two positions, the change in the angular emission function of the lamp is negligible we can write the two following Equations.

$$E_{v1} \approx \frac{I\cos(\theta)}{(H-h)^2+d^2} \quad (7)$$

$$E_{v1}{}' \approx \frac{I\cos(\theta')}{(H-h)^2+d^2+D^2} \quad (8)$$

Where I is a constant and $E_{v1}{}'$ is the illuminance falling on sensor #1 at $t = t'$ and θ' is the nadir angle from the source to the sensor at $t = t'$. To be valid one should use a relatively small value of D compared to the source distance or a source having a very low change in its emission function along the street direction. We assume that the emission function is constant.

Taking the ratio of Equation 7 over 8 we get:

$$\frac{E_{v1}}{E_{v1}{}'} = \frac{\cos(\theta)((H-h)^2+d^2+D^2)}{\cos(\theta')((H-h)^2+d^2)} \quad (9)$$

We can write the two cosines as follow.

$$\cos(\theta) = \frac{H-h}{\sqrt{(H-h)^2+d^2}} \quad (10)$$

$$\cos(\theta') = \frac{H-h}{\sqrt{(H-h)^2+d^2+D^2}} \quad (11)$$

By combining Equations 9, 10 and 11, we can write the following Equation.

$$\frac{E_{v1}}{E_{v1}{}'} = \left(\frac{(H-h)^2+d^2+D^2}{(H-h)^2+d^2}\right)^{3/2} \quad (12)$$

If we replace $(H-h)$ in Equation 12 with Equation 6 we can write the following equation.

$$\frac{E_{v1}}{E_{v1}{}'} = \left(\frac{(\frac{E_{v1}d}{E_{v3}})^2+d^2+D^2}{(\frac{E_{v1}d}{E_{v3}})^2+d^2}\right)^{3/2} \quad (13)$$

After some manipulations, we can find an expression for d which is the horizontal distance between the LANcube v2 and the source normal to the street at t.

$$d = \frac{D}{\sqrt{(\frac{E_{v1}}{E_{v1}{}'})^{2/3}((\frac{E_{v1}}{E_{v3}})^2+1)-(\frac{E_{v1}}{E_{v3}})^2-1}} \quad (14)$$

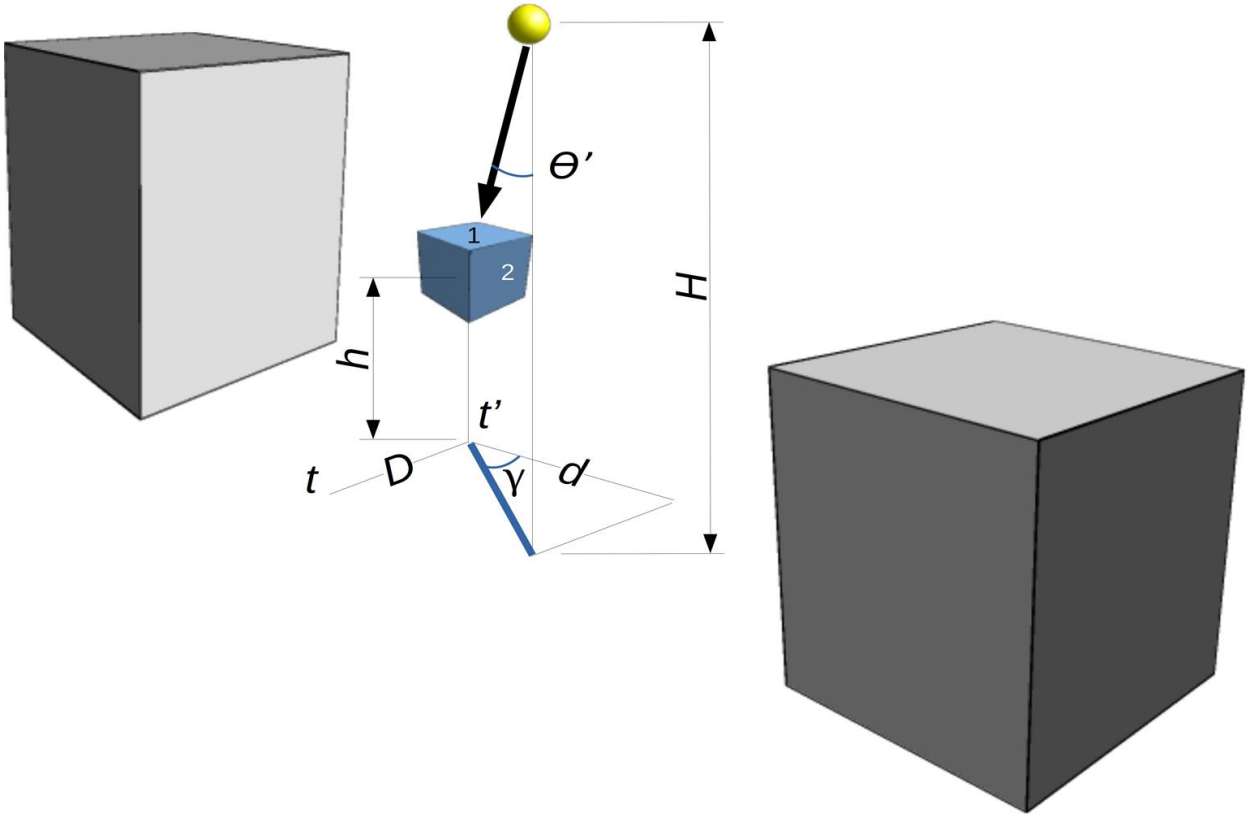

Figure 5. The geometry of an acquisition after the local maximum when the LANcube v2 moved by a distance *D* along the street.

We will see in a later section how *D* can be determined out of the latitude-longitude coordinates of the two corresponding LANcube v2 positions.

Knowing the value of *d* we can now determine the height of the source relative to the ground (H) by using Equation 6.

$$H = d\frac{E_{v1}}{E_{v3}} + h \quad (15)$$

With Equations 2 and 10 we can determine the illuminance normal to the line between the LANcube v2 and the source.

$$E_{v\perp} = \frac{E_{v1}}{\cos(\theta)} = \frac{E_{v1}\sqrt{(H-h)^2+d^2}}{H-h} \quad (16)$$

3.5 Case 2: Lighting device directly above the LANcube v2

This situation happens when only a maximum is detected on sensor #1. If the LANcube v2 moved of a distance D along the street in time t' and that between the two positions, the change in the angular emission function of the lamp is negligible we can write the two following equations.

$$E_{v1} \approx \frac{I}{(H-h)^2} \quad (17)$$

$$E_{v1}{}' \approx \frac{I\cos(\phi')}{(H-h)^2+D^2} \quad (18)$$

Similarly to Equation 11, $\cos(\phi')$ can be expressed as follows.

$$\cos(\phi') = \frac{H-h}{\sqrt{(H-h)^2+D^2}} \quad (19)$$

Combining Equations 17, 18 and 19 we obtain the following relationship between $E_{v1}{}'$ and E_{v1}.

$$\frac{E_{v1}{}'}{E_{v1}} = \left(\frac{(H-h)^3}{((H-h)^2+D^2)^{3/2}}\right) \quad (20)$$

After some manipulations we obtain.

$$H = \frac{D\left(\frac{E_{v1}{}'}{E_{v1}}\right)^{1/3}}{\sqrt{1-\left(\frac{E_{v1}{}'}{E_{v1}}\right)^{2/3}}+h} \quad (21)$$

In that case $d = 0$.

We can easily determine the illuminance normal to the line between the LANcube v2 and the source.

$$E_{v\perp} = E_{v1} \quad (22)$$

3.6 Case 3: lighting device at LANcube v2 height on the side

We can assume that a source is located at or below the LANcube v2 height h on the side when a maximum is only detected on $|E_{v3}|$. In such a case we assume that the source is at the LANcube v2 height. Assuming again that the LANcube v2 moved of a distance D along the street in time t' and that between the two positions, the change in the angular emission function of the lamp is negligible we can write the two following equations.

$$E_{v3} \approx \frac{I}{(d)^2} \quad (23)$$

$$E_{v3}{}' \approx \frac{I\cos(\phi'')}{d^2+D^2} \quad (24)$$

Similarly to Equation 11, $\cos(\phi'')$ can be expressed as follows.

$$\cos(\phi'') = \frac{d}{\sqrt{d^2+D^2}} \quad (25)$$

Combining Equations 23, 24 and 25 we obtain the following relationship between $E_{v3}{}'$ and E_{v3}.

$$\frac{E_{v3}{}'}{E_{v3}} = \frac{d^3}{(d^2+D^2)^{3/2}} \quad (26)$$

After some manipulations we obtain.

$$d = \frac{D\left(\frac{E_{v3}{}'}{E_{v3}}\right)^{1/3}}{\sqrt{1-\left(\frac{E_{v3}{}'}{E_{v3}}\right)^{2/3}}} \quad (27)$$

In that case we assume $H = h$.

We can determine the illuminance perpendicular to the line between the LANcube v2 and the source.

$$E_{v\perp} = E_{v3} \quad (28)$$

3.7 Estimating the luminous flux

We get a rough estimate of the luminous flux of the source (Φ_v) assuming an upward light output ratio (u) and a conversion constant K.

$$\Phi_v \approx \frac{2\pi K E_{v\perp}(d^2+(H-h)^2)}{(1-u)} \quad (29)$$

The value u is determined per spectral types as indicated in Table 1. These numbers can be modified by the user according to the typical local properties of the sources.

The K constant can be estimated after using many in situ measurements for source with known flux. This constant is directly related to the photometric type of the source and to the detection point relative to the source position.

Our goal here is not to determine accurately the luminous flux, but rather to estimate it roughly. We verified, with IESNA files of some usual type III streetlights, that $K = 1$ is a reasonably good choice.

3.8 Converting distance to latitude and longitude and vice versa

The LANcube v2 record the latitude (ϕ) and the longitude (λ) at every acquisition. For that reason, we must be able to convert the distance to the source in term of its latitude and longitude. To accomplish that, we need to convert (ϕ, λ) of the local maximum into (x, y) in meter and then determine (x_l, y_l) the position of the source in that reference system. Then, once defined we can go back to the (ϕ_l, λ_l) position in the latitude-longitude system.

A change in $x$or $y$coordinates can be defined respectively as Δx and Δy.

$$\Delta y = y' - y \approx \frac{\pi}{180} R \Delta\phi \quad (30)$$

$$\Delta x = x' - x \approx \frac{\pi}{180} R \Delta\lambda cos(\phi) \quad (31)$$

Where $\Delta\phi = \phi' - \phi$ and $\Delta\lambda = \lambda' - \lambda$ are respectively variations in latitude and longitude. In Equations 30 and 31, R is the radius of the earth (6 373 000 m).

In the special case where Δx and Δy are the displacement between the positions of the LANcube v2 at t and t', the distance along the path of the LANcube v2 D is given by Equation 32.

$$D = \sqrt{\Delta x^2 + \Delta y^2} \quad (32)$$

One can combine Equation 30 with Equations 31 and 32 to determine D as a function of the variations in latitude and longitude between times t and t'.

The unit vector components defining the displacement of the LANcube v2 between t and t' can be determined with Equations 30 and 31.

$$\hat{X} = \frac{(\lambda\prime - \lambda)\cos(\phi)}{\sqrt{((\lambda\prime - \lambda)\cos(\phi))^2 + (\phi\prime - \phi)^2}} \quad (33)$$

$$\hat{Y} = \frac{(\phi\prime - \phi)}{\sqrt{((\lambda\prime - \lambda)\cos(\phi))^2 + (\phi\prime - \phi)^2}} \quad (34)$$

This unit vector can be converted into the unit vector toward the source from position at t simply by rotating of $\epsilon = -\pi/2$ for a source located to on the right side or $\epsilon = \pi/2$on the left side.

$$\hat{x} = \hat{X}\cos(\epsilon) - \hat{Y}\sin(\epsilon) = -\hat{Y}\sin(\epsilon) \quad (35)$$

$$\hat{y} = \hat{X}\sin(\epsilon) + \hat{Y}\cos(\epsilon) = \hat{X}\sin(\epsilon) \quad (36)$$

Considering that the source is at a distance$d$from the point of maximum illuminance (x, y), we can express the position of the source x_l and y_l.

$$x_l = d\hat{x} + x \quad (37)$$

$$y_l = d\hat{y} + y \quad (38)$$

This displacement can be converted back to changes in latitude and longitude with Equations 30 and 31 and then find the geographical co-ordinates of the source (ϕ_l, λ_l).

$$\lambda_l = \frac{180(x_l - x)}{\pi R\cos(\phi)} + \lambda = \frac{180\hat{x}d}{\pi R\cos(\phi)} + \lambda \quad (39)$$

$$\phi_l = \frac{180(y_l - y)}{\pi R} + \phi \quad (40)$$

3.9 Improving the data with local statistics

We assume that the emission function does not change significantly between t and t'. Such assumption can result

in errors in source position and height, which reflect in the evaluation of the luminous flux. Another factor that can introduce errors is the blocking of the light by canopy or other smooth obstacles. Generally, the error translates in incredibly high luminous fluxes along with large lamp heights. One manner to correct for these errors is to analyze height distribution of nearby sources. Then we assume that the incorrect lamp is likely to be at the most common height of nearby lamps that are significantly higher than the LANcube v2 (we set a threshold at 4 m to exclude the car headlights and residential lights). Then we change the erroneously detected height to the most common nearby value. The corresponding positions and luminous flux may be re-scaled to that new assigned height (H'). If we define the initially determined height, distance, and luminous flux as H, d and Φ_v, the new values ($d'$and Φ') are computed with Equations 41 and 42.

$$d' = d\frac{H\prime - h}{H - h} \quad (41)$$

$$\Phi'_v = \Phi_v\left(\frac{H\prime - h}{H - h}\right)^2 \quad (42)$$

4 Results and discussion

After applying the method described above, we obtain an approximate lighting device inventory for the places where we roam with the LANcube v2 on top of a car. When examining that inventory, we noticed sources having flux lower than 250 lumens, which is not expected since typical residential light bulbs have about 400 to 500 lumens. After a closer analysis, we found that these very low sources often correspond to road panel signs. So, they are the light of a nearby streetlight reflected in the panel. For that reason, we are removing all sources having a luminous flux lower than 250 lumens. Figures 6, 7 and 8 show the results for two villages located in the province of Québec, Canada. The inventory extracted contains the latitude and longitude, height relative to the ground, luminous flux, and the spectral type. At a first glance we can notice that the different municipal administration delivers very different lighting practices. In Saint-Camille, most sources are HPS with relatively low luminous flux, most of them being below 4000 lumens. On the opposite, in Stoke we see that the dominant technology is LED at 4000K and most flux is higher than 6000 lumens. It is noticeable that Stoke replaced their HPS lamps for 4000K LED some years ago and when looking to the few remaining HPS, the new flux is generally more than ten times the old HPS ones. Of course, we know that HPS fluxes decrease significantly with time and that in these small villages no maintenance protocols are implemented, the HPS bulbs being replaced only when they no longer light up.

(a) (b)

Figure 6. Detected spectral types and luminous fluxes in Saint-Camille, Québec, Canada.

(a) (b)

Figure 7. Detected spectral types and luminous fluxes in central part of Saint-Camille, Québec, Canada.

(a) (b)

Figure 8. Detected spectral types and luminous fluxes in Stoke, Québec, Canada.

To evaluate the performance of the method, it is important to compare the extracted inventory with the ground truth. We performed that comparison on the height and the spectral type extracted. We excluded the luminous flux from that comparison simply because we do not know that information from the ground truth inventory. We also compared the detection success defined as the number of detected sources within a buffer distance of 17 meters from the position of the devices included in the ground truth inventory. In this latter comparison, we do not care if the method correctly determined the technology and height, we only focus on the position. The buffer distance was determined based on the typical detection distance away from the LANcube v2 position. 17 m may appear large, but the GPS accuracy during the sampling is of the order of 8 meters and at 50 km/h, we only have a measurement point every 9 meters. Combination of the two uncertainty gives ≈ 18m which is coherent with 17 m buffer used. To confirm the significance of that buffer distance, we compared the position of the same set of sources as detected during two consecutive detection experiments. This gives an average error of 12 meters with a dispersion around that value having a standard deviation of 7 meters, i.e., 19 m. This is like the buffer distance. To exclude multiple detection of the same source, we merged the detected lighting systems of the same spectral type. The merge is only performed when the sources are detected at least 20 seconds of interval from each other (i.e., two different paths). In such case, the position, height, and luminous flux of the merged device is set as the average of the original values. The maximum distance for the merging of two sources was set to 25 m which is in our case the minimum distance between two similar streetlights in the villages. This value can be changed for other territories as it is a parameter of the script input file. In our case we tried different values to find that one to give the best results. In any case according to our localization accuracy at 50 km/h, this number should not be lower than 17 m or 13 m at 25 km/h. The average distance between streetlights in the village center is ≈ 60m while it lies between 120 m and 1 km out of the village center. One major advantage of the merging process is that one can perform many consecutive scans of a road to increase the accuracy of the inventory.

In Saint-Camille and Stoke, no lighting systems were detected farther than 25 m off the road. Most of the lighting systems were detected within 15 m from the road.

In addition to streetlights and some private parking lights, 48 private lights were detected in the two villages. Most of them are small residential bulbs installed on house and building facades typically at lower heights compared to streetlights (less than 4 m). We excluded the lower heights private lights from the ground truth comparison because it was almost impossible to validate where they are located and if they were on or off during the sampling experiment.

Table 2 shows the results of the comparison between the values detected by the LANcube v2 and the ground truth. Only one source out of 74 was not detected by the LANcube v2 (3%). It is in a zone where the car speed was higher than 75 km/h. In such case, the distance between two consecutive measurements is around 12 meters, so that it is possible that the illuminance decrease was so high that the source was simply ignored. With such a large distance between points, the validity of an almost constant angular emission function is clearly faulty anyway. Actually, for such a reason, we suggest limiting the driving speed to around 25 km/h when performing a lighting device inventory with the LANcube v2. At 25 km/h the distance between points is about 4 m.

For the determination of the height of the lighting system, we generally overestimate the real height (see Table 1). The overestimation is higher for LED than for HID system and this is clearly because of the very different emission functions. Apparently, the HID meets in a better way the assumption that the angular emission function is constant. There is no obvious way to correct that overestimation except if the further experiments shows that the overestimate is very well linked to the lighting technology. We do not have enough data to confirm this yet.

The success in spectral type recognition is high. We confused only one source out of 74 ($\approx 1\%$). We detected one HPS as a 3000K LED. HPS detection is a challenge since the very large dispersion in the 3D color space (see Figure 2). Moreover, 3000K LEDs are next to the HPS region in the color space. We were probably sampling an especially white HPS lamp. For that reason, we need to sample more HPS lamps to improve the spectral recognition table 1.

Table 2. Detection statistics for sources higher than 4 m within 15 m from the road. We considered mainly the streetlights and some private industrial lights in Saint-Camille and Stoke.

Parameter	**Value**	**Percentage**
Sources detected	73/74	98.6%
Not detected	1/74	1.4%
False detection	0	0%
Spectrum recognized	73/74	98.6%
Height error >200%	4/74	5.4%
Averaged height error	HID cobra	+21%±32%
and standard deviation	LED	+53%±50%

We succeed in detecting asymmetric sources like wall packs installed on building facades perpendicular to the road along with billboards. Car headlights and spotlights are detected by the LANcube v2 but the determination of their distances and then of their fluxes is completely off the reality. This is because that their angular function is far from constant, so that we systematically overestimate their distance by about 1 order of magnitude. Such a large distance combined with a normal illuminance detected end up in fluxes about 3 orders of magnitude too high. For the moment, we exclude these tremendous fluxes from the extracted inventory.

5 Conclusion

In this paper, we suggest a new method to determine the lighting devices inventory of a region out of the data acquired with the LANcube v2 radiometer. The method can detect $\sim 99\%$of the high flux sources (e.g.,$\gtrapprox 1000$ lumens) located within 15 m from the road. The method also detects small flux sources like residential bulbs if they are not too far from the road. That method offers the advantage to detect also private lights that are never included in public lighting inventories. The method is very efficient to recognize the spectral type of each source. On the other hand, the method generally overestimates in average the lamp heights by 21 to 53 percent, depending on the angular photometry of the lamp. It most probably also overestimates the associated lamp fluxes. The height overestimate is the direct consequence of one basic assumption of the method that the angular emission function of the sources is constant between two consecutive detection points. Errors in detection may also happen because of the presence of smooth obstacles like tree leaves. For that reason, we recommend performing LANcube v2 inventory in Autumn when the leaves have fallen. The proposed methodology does not allow the correct determination of the distance of spotlights because of their highly variable and focused angular emission function.

Despite the problems associated with this method, we believe that it constitutes a powerful tool for the study of direct ALAN and its effects. Its application is not restricted to roads and streets. As an example, the LANcube v2 may be attached to a helmet so that a pedestrian or a cyclist can record with very high accuracy the ALAN and even in places inaccessible to cars.

Acknowledgements

We applied the sequence-determines-credit approach for the sequence of authors [15]. This research was supported by Fonds de recherche du Québec Nature et technologies (FRQNT) and by Fonds de recherche du Québec Santé. We want to thank Alexandre Simoneau, who helped with the python code writing. We finally want to thank Élysé Lapalme who contributed to the development of the LANcube v2 control software.

References

[1] Boldogh, S.; Dobrosi, D.; Samu, P. The effects of the illumination of buildings on house-dwelling bats and its conservation consequences. Acta Chiropterologica 2007, 9, 527–534.

[2] Kamrowski, R.L.; Limpus, C.; Pendoley, K.; Hamann, M. Influence of industrial light pollution on the sea-finding behaviour of flatback turtle hatchlings. Wildlife Research 2015, 41, 421–434.

[3] Brüning, A.; Hölker, F.; Wolter, C. Artificial light at night: implications for early life stages development in four temperate freshwater fish species. Aquatic Sciences 2011, 73, 143–152.

[4] Da Silva, A.; Valcu, M.; Kempenaers, B. Light pollution alters the phenology of dawn and dusk singing in common European songbirds. Philosophical Transactions of the Royal Society of London B: Biological Sciences 2015, 370, 1–2.

[5] Briggs, W.R. Physiology of plant responses to artificial lighting. Ecological consequences of artificial night lighting 2006, pp. 281–304.

[6] Garcia-Saenz, A.; Sánchez de Miguel, A.; Espinosa, A.; Valentin, A.; Aragonés, N.; Llorca, J.; Amiano, P.; Martín Sánchez, V.; Guevara, M.; Capelo, R.; others. Evaluating the association between artificial light-at-night exposure and breast and prostate cancer risk in Spain (MCC-Spain study). Environmental health perspectives 2018, 126, 047011.

[7] Garcia-Saenz, A.; de Miguel, A.S.; Espinosa, A.; Costas, L.; Aragonés, N.; Tonne, C.; Moreno, V.; Pérez-Gómez, B.; Valentin, A.; Pollán, M.; others. Association between outdoor light-at-night exposure and colorectal cancer in Spain. Epidemiology 2020, 31, 718–727.

[8] Hänel, A., Posch, T., Ribas, S. J., Aubé, M., Duriscoe, D., Jechow, A., ... & Kyba, C. C. (2018). Measuring night sky brightness: methods and challenges. *Journal of Quantitative Spectroscopy and Radiative Transfer*, *205*, 278-290.

[9] Longcore, T., Rodríguez, A., Witherington, B., Penniman, J. F., Herf, L., & Herf, M. (2018). Rapid assessment of lamp spectrum to quantify ecological effects of light at night. *Journal of Experimental Zoology Part A: Ecological and Integrative Physiology*, *329*(8-9), 511-521.

[10] Aubé, M., Roby, J., & Kocifaj, M. (2013). Evaluating potential spectral impacts of various artificial lights on melatonin suppression, photosynthesis, and star visibility. *PloS one*, *8*(7), e67798.

[11] Bennie, J., Davies, T. W., Cruse, D., & Gaston, K. J. (2016). Ecological effects of artificial light at night on wild plants. *Journal of Ecology*, *104*(3), 611-620.

[12] Aubé, M.; Marseille, C.; Farkouh, A.; Dufour, A.; Simoneau, A.; Zamorano, J.; Roby, J.; Tapia, C. Mapping the Melatonin Suppression, Star Light and Induced Photosynthesis Indices with the LANcube. Remote Sensing 2020, 12, 3954.

[13] Aubé, M. Online LANcube documentation., http://dome.obsand.org:2080/wiki/index.php/Prof/LANcube, 2023.

[14] Aubé, M., Houle, J. P., Desmarais, J., Veilleux, N., & Bordeleau, É. (2021). Modeling the Spectral Properties of Obtrusive Light Incident on a Window: Application to Montréal, Canada. *Remote Sensing*, *13*(14), 2767.

[15] Tscharntke, T.; Hochberg, M.E.; Rand, T.A.; Resh, V.H.; Krauss, J. Author sequence and credit for contributions in multiauthored publications. PLoS biology 2007, 5, e18.